Epilepsia, **(*):1–10, 2008
doi: 10.1111/j.1528-1167.2008.01881.x

FULL-LENGTH ORIGINAL RESEARCH

Three-dimensional hippocampal atrophy maps distinguish two common temporal lobe seizure–onset patterns

*Jennifer A. Ogren, †‡Anatol Bragin, †‡Charles L. Wilson, †Gil D. Hoftman, §Jack J. Lin, ¶Rebecca A. Dutton, †Tony A. Fields, †¶Arthur W. Toga, †‡¶Paul M. Thompson, *†‡#Jerome Engel, Jr., and †Richard J. Staba

*Department of Neurobiology, David Geffen School of Medicine at UCLA, Los Angeles, California, U.S.A.; †Department of Neurology, David Geffen School of Medicine at UCLA, Los Angeles, California, U.S.A.; ‡Brain Research Institute, David Geffen School of Medicine at UCLA, Los Angeles, California, U.S.A.; §Department of Neurology, UCI School of Medicine, Irvine, California, U.S.A.; ¶Laboratory of Neuro Imaging (LONI), David Geffen School of Medicine at UCLA, Los Angeles, California, U.S.A.; and #Department of Psychiatry and Biobehavioral Sciences, David Geffen School of Medicine at UCLA, Los Angeles, California, U.S.A.

Summary

Purpose: Current evidence suggests that the mechanisms underlying depth electrode–recorded seizures beginning with hypersynchronous (HYP) onset patterns are functionally distinct from those giving rise to low-voltage fast (LVF) onset seizures. However, both groups have been associated with hippocampal atrophy (HA), indicating a need to clarify the anatomic correlates of each ictal onset type. We used three-dimensional (3D) hippocampal mapping to quantify HA and determine whether each onset group exhibited a unique distribution of atrophy consistent with the functional differences that distinguish the two onset morphologies.

Methods: Sixteen nonconsecutive patients with medically refractory epilepsy were assigned to HYP or LVF groups according to ictal onset patterns recorded with intracranial depth electrodes. Using preimplant magnetic resonance imaging (MRI), levels of volumetrically defined HA were determined by comparison with matched controls, and the distribution of local atrophy was mapped onto 3D hippocampal surface models.

Results: HYP and LVF groups exhibited significant and equivalent levels of HA ipsilateral to seizure onset. Patients with LVF onset seizures also showed significant contralateral volume reductions. On ipsilateral contour maps HYP patients exhibited an atrophy pattern consistent with classical hippocampal sclerosis (HS), whereas LVF atrophy was distributed more laterally and diffusely. Contralateral LVF maps also showed regions of subicular atrophy.

Discussion: The HS-like distribution of atrophy and the restriction of HA to the ipsilateral hippocampus in HYP patients are consistent with focal hippocampal onsets, and suggest a mechanism utilizing intrahippocampal circuitry. In contrast, the bilateral distribution of nonspecific atrophy in the LVF group may reflect mechanisms involving both hippocampal and extrahippocampal networks.

KEY WORDS: Hippocampal sclerosis, MRI, Temporal lobe epilepsy.

Intracranial depth electrode recordings indicate that the majority of seizures in patients with temporal lobe epilepsy (TLE) may be segregated into two groups based on electrographic ictal onset patterns (Engel, 1990). Hypersynchronous (HYP) onsets consist of long-lasting (>5-s) trains of low-frequency (<2-Hz), high-amplitude spikes, whereas low-voltage fast (LVF) onsets are characterized

Accepted August 22, 2008; Early View publication xxxxx.
Address correspondence to Dr. Richard J. Staba, Department of Neurology, David Geffen School of Medicine at UCLA, 710 Westwood Plaza, Los Angeles, CA 90095-7169, U.S.A. E-mail: rstaba@mednet.ucla.edu

Wiley Periodicals, Inc.

by high-frequency, low-amplitude activity (Townsend & Engel, 1991; Spencer et al., 1992a; Velasco et al., 2000; Bragin et al., 2005b). Seizures beginning with HYP onsets are more likely to originate focally in hippocampal regions and are less likely to spread quickly to the contralateral hemisphere. In contrast, LVF onset seizures are more likely to be regional as opposed to focal, tend to propagate quickly to the contralateral hemisphere, and often originate in the neocortex (Lieb et al., 1981; Engel, 1990; Townsend & Engel, 1991; Spanedda et al., 1997; Velasco et al., 2000). These differences in ictal-onset morphology, propagation time, and spatial distribution, as well as differences in voltage-depth profiles (Bragin et al., 2005b) indicate that seizures with HYP onsets arise via different mechanisms than those beginning with LVF onsets.

Despite the differences between HYP and LVF seizure onsets, a characteristic common to these onset patterns is the presence of hippocampal sclerosis (HS) and/or hippocampal atrophy (HA) ipsilateral to the epileptogenic region (Townsend & Engel, 1991; Spencer et al., 1992b; Spanedda et al., 1997; Velasco et al., 2000). However, if different mechanisms of seizure generation and propagation underlie the two onset morphologies, distinct patterns of anatomic damage might be expected for each group. Although previous studies used cell counts to quantify the extent of HS in patients with HYP or LVF onsets, histologic analysis has been derived largely from surgically resected tissue rather than autopsy specimens, so only ipsilateral hippocampus is available and often it is incomplete. It has long been known that damage to contralateral structures may be present as well (Margerison & Corsellis, 1966; Mathern et al., 1995b), and thus HA may be present contralaterally and may differ in extent depending on seizure-onset type.

To fully characterize the extent of damage associated with each onset morphology, it is necessary to quantify HA in the entire hippocampus bilaterally. Characterization of the spatial distribution of atrophy in HYP and LVF patients may indicate networks involved in seizure genesis. Recently developed noninvasive magnetic resonance imaging (MRI)–based neuroimaging techniques have been shown to be highly sensitive in detecting and mapping local areas of HA throughout the hippocampi of patients with Alzheimer's disease (Thompson et al., 2004; Apostolova et al., 2006; Frisoni et al., 2006), schizophrenia (Narr et al., 2004), autism (Nicolson et al., 2006), depression (Ballmaier et al., 2008), bipolar illness (Bearden et al., 2007), blindness (Lepore et al., 2008), and TLE (Hogan et al., 2004; Lin et al., 2005). Using techniques such as those developed by Thompson et al. (1996, 2004), three-dimensional (3D) hippocampal surface models may be derived from manually traced serial MRI sections, providing detailed maps of local hippocampal thickness measurements. Maps from patients and from healthy control subjects may then be compared, to quantify atrophy and evaluate the distribution of tissue loss associated with a particular patient group.

In the present study, patients with medically refractory TLE were assigned to HYP and LVF onset groups based on ictal-onset patterns recorded with intracranial depth electrodes. Surface contour maps of hippocampi ipsilateral and contralateral to ictal onset were generated for patients with TLE and for age- and gender-matched control subjects to determine the extent and distribution of HA in each seizure-onset group. We hypothesized that this approach would reveal distinct atrophy profiles for each seizure-onset pattern.

Methods

Subjects

Subjects were patients with medically intractable complex partial seizures of probable temporal lobe origin, who required depth electrodes in order to localize brain area(s) of seizure onset (Crandall et al., 1963; Fried et al., 1999). All patients gave written informed consent prior to participating in these research studies, which were approved by the UCLA Office for Protection of Research Subjects Medical Institutional Review Board.

Each patient was surgically implanted with 8–14 clinical depth electrodes that were positioned using stereotactic coordinates. Electrodes were 1.25-mm diameter flexible polyurethane seven-contact clinical depth electrodes (AdTech Medical Instruments, Racine, WI, U.S.A.), inserted orthogonally and positioned within clinically relevant areas. Patients underwent videotelemetry monitoring 24 h a day to locate brain areas where spontaneous seizure activity began (Engel, 1996b). Intracranial EEG was acquired at a sampling rate of 200 Hz and a bandwidth of 0.1–70 Hz using a Telefactor monitoring system (Astro-Med, Inc., West Warwick, RI, U.S.A.). Attending neurologists in the UCLA Seizure Disorders Center identified locations of electrographic seizure onset based on the recording of multiple, independent, spontaneous seizure occurrences during an average of 1–3 weeks that patients were in the hospital.

Subjects included in the present study were selected from a set of patients who participated in a previous study (Bragin et al., 2005b). Because the objective of this study was to contrast hippocampal atrophy in patients with HYP or LVF ictal onset patterns, patients were included if they had only one type of ictal onset pattern, that is, HYP or LVF, and if a complete axial T_1-weighted MR image dataset was available. Using these criteria, 16 nonconsecutive, surgical epilepsy patients were included in the present study from a total of 21 patients used in the previous study.

Seizure-onset classification

Classification of intracranial ictal EEG corresponding to patients used in this study was performed by three

investigators (AB, CW, and JE) as part of an analysis from a previous study (Bragin et al., 2005b). Briefly, sixty-one seizures from 16 patients (median seizures per patient 3, range between 2 and 7) were visually reviewed to determine ictal-onset morphology. Classification of ictal-onset patterns was based on the following criteria (Velasco et al., 2000): ictal onsets labeled ''hypersynchronous'' (HYP) consisted of rhythmic, high amplitude spikes <2 Hz that lasted >5 s, whereas onsets labeled ''low-voltage fast'' (LVF) consisted of low amplitude EEG >10 Hz. On the basis of these seizure-onset criteria, seven patients (four female) were assigned to the HYP ictal-onset group, whereas the nine remaining patients (six female) comprised the LVF group.

Neuroimage processing

Preoperative MRI scans were acquired using a 1.5T Siemens Sonata full-body scanner with head coil (Siemens Medical Solutions USA, Malvern, PA, U.S.A.). Each 3D T_1-weighted image series was acquired in the axial plane using an SPGR or MPRAGE sequence, with a $256 \times 256 \times 124$ matrix that produced 1-mm isotropic voxels. Using the same imaging protocol on a different 1.5T MR scanner, equivalent MRI scans were acquired from nonepileptic healthy control subjects who were selected based on age and gender to match each individual patient (mean age ± SD, in years; HYP patients: 32.9 ± 11, controls: 29.5 ± 4.5; LVF patients: 38.5 ± 6.4, controls: 31.8 ± 3.3). To compensate for head tilt, alignment, and overall differences in brain size between subjects, each MRI dataset was linearly registered to the ICBM53 average brain template (International Consortium for Brain Mapping) using semi-automated registration software (Collins et al., 1994) and nine-parameter global scaling. This transformation into standardized space allowed for direct comparison between subjects.

Normalized MRI datasets were resliced in the coronal plane, and hippocampal boundaries were manually traced by a single investigator (JO) according to an established protocol (Watson et al., 1992) to include the subiculum, presubiculum, dentate gyrus, and hippocampus proper. The protocol was modified for the most posterior portions of the hippocampal tail, which were delineated on the basis of a standard neuroanatomic atlas (Mai et al., 2004). During tracing procedures, the investigator was blind to each patient's seizure onset type and hemisphere of onset. Reliability of the tracing protocol was evaluated using a single measurement, model 2 intraclass correlation (ICC) (Portney & Watkins, 2008) computed from an analysis of variance (ANOVA) on whole hippocampal volumes (n = 7) derived from tracings performed by the first investigator and a second investigator (GH). Results indicated strong agreement between investigators to the tracing protocol with little difference in whole volumes (ICC = 0.95, F = 0.13). Prior to processing, traces were separated into two patient (HYP and LVF) and two control (CTL-HYP and CTL-LVF) groups. From each series of hippocampal traces a 3D parametric surface mesh model was created using established modeling methods (Thompson et al., 2004) (Fig. 1). Each 3D hippocampal mesh model consisted of a lattice-like network of an equivalent number of points. The surface distribution of these points was spatially normalized, allowing subsequent comparison of hippocampal models on a point-by-point basis (Fig. 1D). Following surface mesh generation, a medial 3D curve was derived for each hippocampus. This imaginary line threads through the hippocampus along its length, connecting the centers of mass at each point along the anterior–posterior axis. The distance from the medial curve to the hippocampal surface, known as radial size, was calculated for each surface point on the mesh models (Fig. 1E).

Data analysis

Patient hippocampi within the hemisphere of seizure onset were labeled ''ipsilateral,'' whereas hippocampi within the hemisphere opposite the side of seizure onset were labeled ''contralateral.'' For patients with bilateral seizure onsets (n = 1), both hippocampi were classified as ipsilateral to seizure onset. To control for any inherent hippocampal asymmetry that might be related to age, gender, or hemisphere, each control subject's hippocampi were classified as ''ipsilateral'' or ''contralateral'' according to the matched patient's hemisphere of seizure onset.

Normalized hippocampal volumes derived from each set of traces, were calculated for each patient and control hippocampus, and group averages were calculated. Paired *t*-tests were used to compare ipsilateral and contralateral hippocampal volumes of each patient group (HYP or LVF) with those of corresponding controls. Relative volume reductions were determined for each patient hippocampus by comparison to controls. Unpaired *t*-tests were used to compare ipsilateral and contralateral volume reductions in the HYP group with those of the LVF group.

To allow calculation and visual depiction of group data, all surface contour maps were oriented in radiologic right space. Radial size values at analogous surface points were averaged across individuals to create 3D hippocampal surface contour maps representing the average shape and size of each group's hippocampi. Statistical ANOVA was used to compare radial size differences between patient and control groups at each hippocampal surface point. The resulting p-values, indicating the significance of local atrophy at each point, were mapped in a color-coded fashion onto the surface of group mean 3D contour maps, illustrating the distribution of areas of significant local atrophy in each seizure-onset group. To correct for multiple comparisons and assign an overall p-value to each P map (Nichols & Holmes, 2002; Thompson et al., 2003), permutation tests (1×10^6 iterations) were used to determine how likely the observed level of significant atrophy

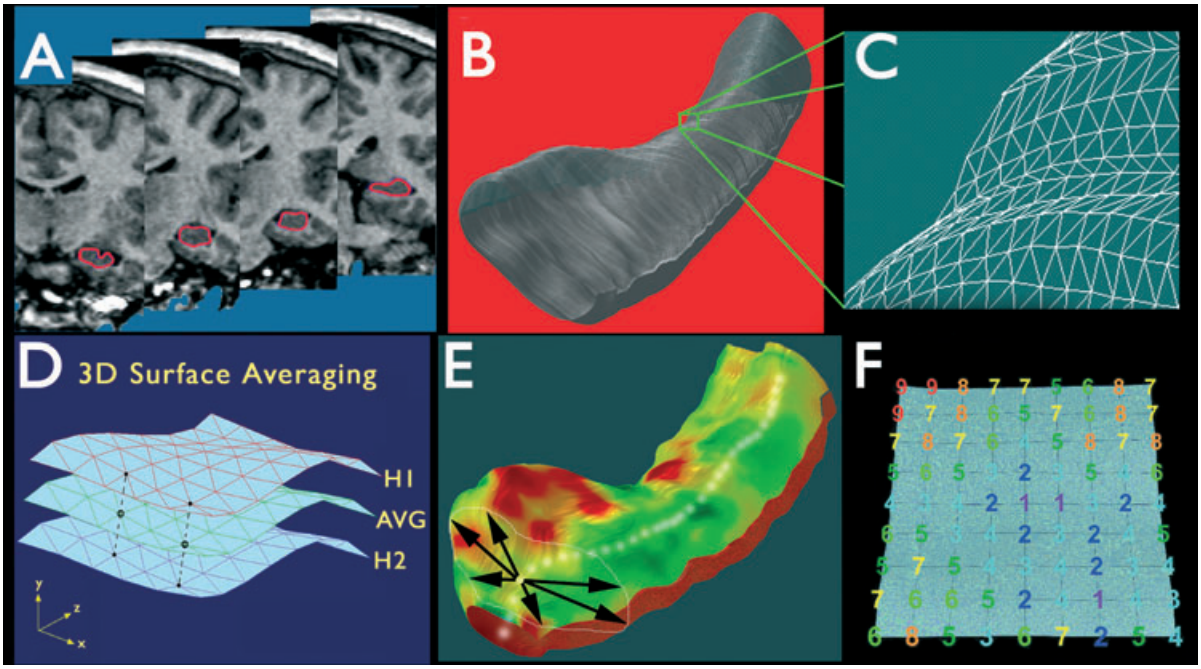

Figure 1.
Steps involved in three-dimensional (3D) hippocampal surface modeling. **(A)** The hippocampus is traced in contiguous coronal magnetic resonance imaging (MRI) slices. **(B, C)** Using anatomic surface modeling software (UCLA Laboratory of NeuroImaging, LONI), traces are converted into a 3D parametric surface. (**D**) Surfaces from patients or controls can be averaged to produce an average anatomic model for each group. (**E**) On the basis of centers of mass of consecutive hippocampal traces, a medial curve is derived for each subject. **(F)** The distance from the medial curve to each surface point (radial size) is then calculated. Adapted from Thompson et al. (2004), with permission.

(proportion of suprathreshold statistics, with the threshold set at $p < 0.01$) within each P map would occur by chance (Thompson et al., 2003, 2004). The number of permutations N was chosen to be 100,000, to control the standard error SE_p of omnibus probability p, which follows a binomial distribution B(N, p) with known standard error (Edgington, 1995). When $N = 8{,}000$, the approximate margin of error [95% confidence interval (CI)] for p is around 5% of p; to further improve upon this, we ran 100,000 permutations, with 0.05 chosen as the significance level.

To further characterize the distribution of atrophy associated with HYP and LVF onset groups, P map surface regions were described in terms of underlying anatomic structures, including Ammon's horn (CA1 through CA4), dentate gyrus (DG), prosubiculum, subiculum, and presubiculum. External features on the hippocampal surface were used to align the 3D maps with structures in a brain atlas (Mai et al., 2004), which was the same human brain atlas used during the tracing process. Changes in hippocampal morphology on the map associated with the end of the uncus on the anterior medial surface and rostral reorientation of the subiculum (and hippocampus) around the longitudinal axis on the posterior medial surface were identified in the coronal plane on the atlas. Superior and inferior surfaces on the map near these external landmarks were labeled with respect to hippocampal subfields depicted in the atlas. Hippocampal areas with complex anatomy, that is, including two or more subfields between the surface and center of the hippocampus, were labeled as multiple subfields. The 3D hippocampal map in Fig. 2 illustrates the approximate surface locations of subfields within anterior, middle, and posterior sections of hippocampus.

Results

Review of ictal discharge patterns recorded from intracranial depth electrodes positioned within temporal lobe areas showed that of the 16 nonconsecutive patients with medically refractory epilepsy used in this study, seven had HYP ictal onsets (Fig. 3A), whereas the remaining nine had LVF ictal onsets (Fig. 3B). Mean [±standard deviation (SD)] seizure frequency prior to depth electrode evaluation was 6.5 ± 5.5 seizures/month in the HYP group, and 5.7 ± 6.9 seizures/month in the LVF group. Mean

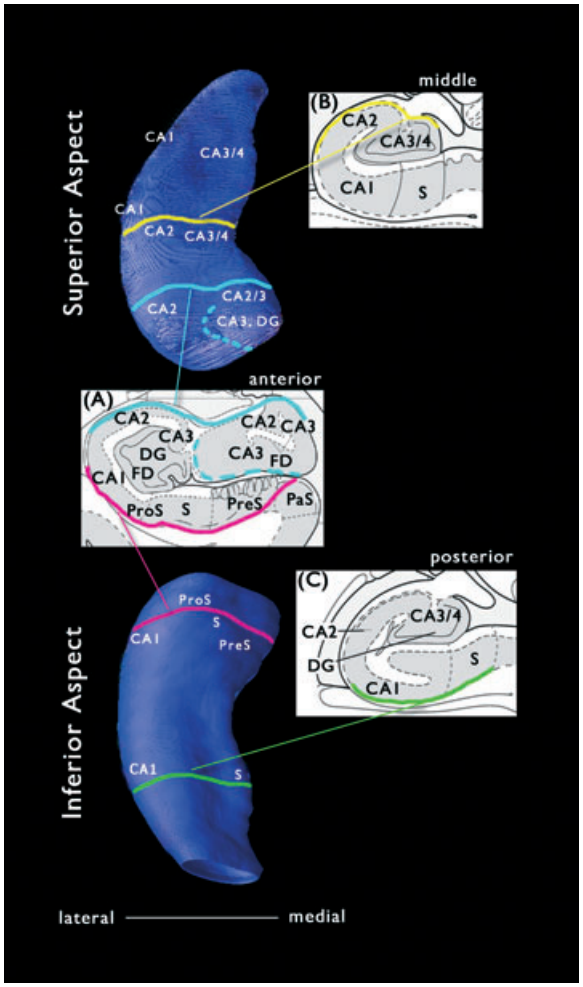

Figure 2.
Contour maps depicting the estimated surface distribution of underlying hippocampal subfields. (Top) Superior aspect of contour map representing a typical hippocampus. (Bottom) Inferior aspect of same hippocampus. (Inset Panels) Hippocampal subfield boundaries depicted in coronal cross-sections through (**A**) anterior, (**B**) middle, and (**C**) posterior hippocampus. CA, cornu ammonis; DG, dentate gyrus; PreS, presubiculum; ProS, prosubiculum; S, subiculum. Inset panels adapted from Mai et al. (2004), with permission.

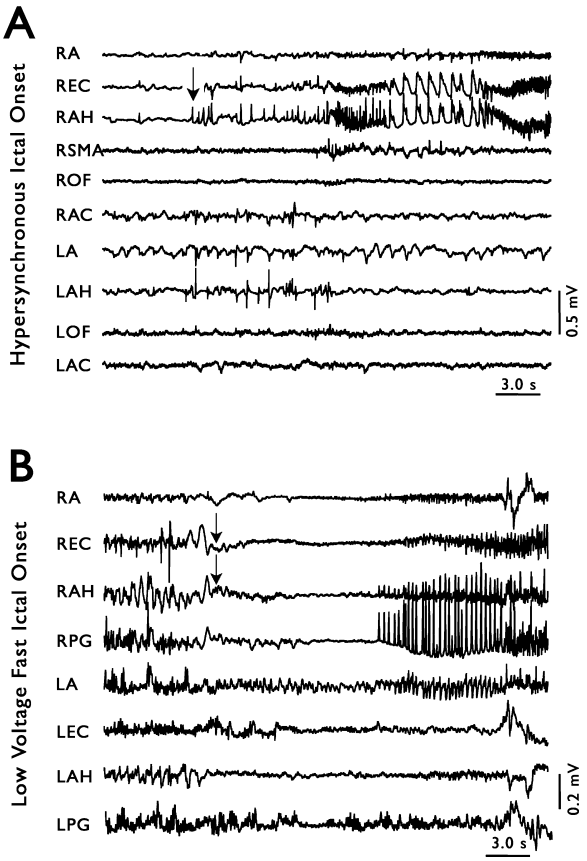

Figure 3.
Two types of seizure onsets recorded intracranially in patients with temporal lobe epilepsy. Arrows indicate seizure onset. (**A**) An example of hypersynchronous (HYP) seizure onset. Note the low frequency, high amplitude spikes just before seizure in RAH, and the failure of the seizure to propagate to regions outside of ipsilateral mesial temporal areas. (**B**) An example of low-voltage fast (LVF) seizure onset. The characteristic high frequency, low amplitude activity is most prominent in REC. Note the rapid involvement of the contralateral amygdala (LA) in the seizure.

duration of epilepsy from age of first epileptic seizure until time of depth electrode evaluation was 21.9 ± 14.3 years for patients with HYP ictal onsets, and 25.4 ± 13.6 years for patients with LVF onsets.

Hippocampal volume analysis

Analysis of patient hippocampal volumes with respect to matched controls showed that HYP and LVF ictal onset groups both had significantly reduced ipsilateral hippocampal volumes (HYP: 2,924 ± 732 mm^3 vs. 3,900 ± 267 mm^3, p = 0.007; LVF: 2,810 ± 528 mm^3 vs. 3,768 ± 343 mm^3, p = 0.001; Fig. 4). There was no significant difference in contralateral volumes between HYP onset patients and controls (3,648 ± 411 mm^3 vs. 3,776 ± 262 mm^3, p = 0.43), but there was a significant reduction in contralateral volume observed in the LVF group (3,408 ± 499 mm^3 vs. 3,882 ± 343 mm^3, p = 0.03). Analysis of volume reductions between HYP and LVF groups showed no significant difference in the

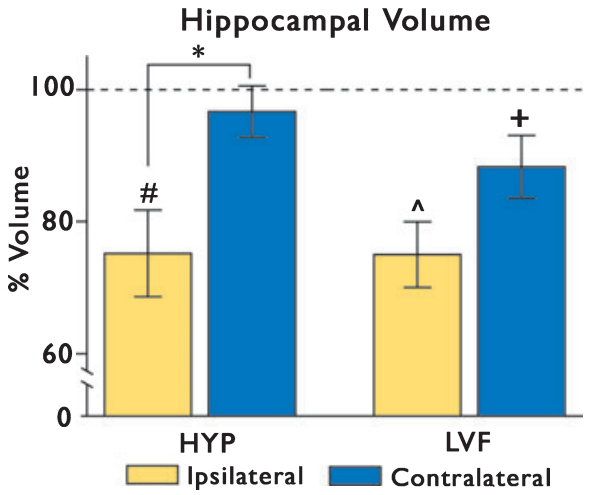

Figure 4.
Hippocampal volume relative to controls. Average patient volumes are expressed as a percentage of corresponding control averages. Note the scale break on the *y*-axis. Hypersynchronous (HYP), left two bars. In the HYP group, ipsilateral hippocampal volumes were significantly smaller than control volumes (#p = 0.007). These ipsilateral volume reductions were significantly greater than those observed contralaterally (*p = 0.02). Low-voltage fast (LVF), right two bars. In the LVF group, ipsilateral hippocampal volumes were significantly smaller than those of corresponding control subjects (^p = 0.001). Contralateral volumes were also significantly reduced relative to controls (+p = 0.03). Ipsilateral volume reductions were not significantly different from contralateral reductions.
Epilepsia © ILAE

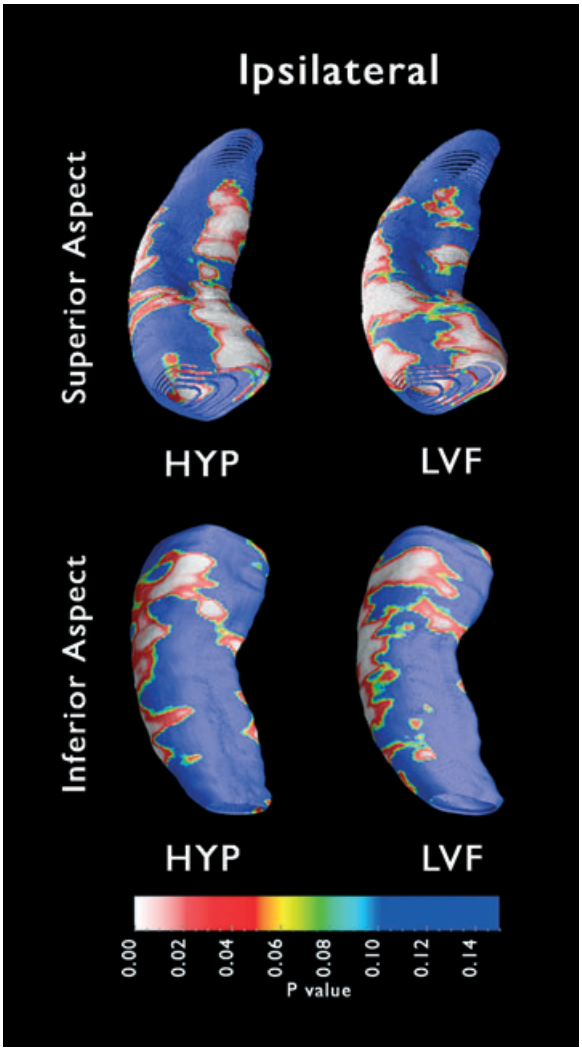

Figure 5.
Structural changes in ipsilateral (epileptogenic) hippocampus: Mapping three-dimensional (3D) hippocampal atrophy. Surface contour maps depicting areas of local atrophy (P maps) show regions of significant differences in HYP (n = 8) and LVF (n = 9) patients relative to controls. White and red indicate areas of significant atrophy (p < 0.05), whereas blue indicates areas without significant atrophy (p > 0.10). The HYP P map (left column) exhibits more medial atrophy, whereas the LVF P map (right column) depicts more extensive lateral atrophy. Significant levels of local atrophy relative to controls were observed in both patient groups (HYP p < 0.015, LVF p < 0.004).
Epilepsia © ILAE

amount of volume loss ipsilateral (unpaired *t*-test, p = 0.98) or contralateral to ictal onset (p = 0.23). Within the HYP group, however, patients had significantly greater hippocampal volume reductions ipsilateral than contralateral to ictal onset (p = 0.02; Fig. 4). In contrast, within the LVF group, there was no significant difference between ipsilateral and contralateral volumes (p = 0.07).

Distribution of hippocampal atrophy

Surface contour maps of color-coded p-values (P maps) showed areas of significant differences between patient and control groups. Regions of significant atrophy depicted on the surface of these P maps were characterized with respect to underlying hippocampal subfields (See Methods, Fig. 2), using a standard neuroanatomic atlas (Mai et al., 2004). Although both onset groups displayed equivalent volume reductions ipsilaterally, P maps revealed two distinct patterns of ipsilateral atrophy. In the ipsilateral hippocampus of the HYP group, atrophy was present in lateral areas of the hippocampus, representing damage in CA1. This area of damage was most prominent on the inferior surface, as was the atrophy of prosubiculum (Fig. 5, bottom left). Examination of the superior surface

of the HYP ipsilateral P map showed an absence of lateral CA2 atrophy and a heavy concentration of atrophy along the medial hippocampus, representing mainly CA3, CA4, and DG.

The LVF ipsilateral P map showed that atrophy was present medially, but more notable damage was distributed in lateral areas (Fig. 5, right column). Based on the locations of hippocampal areas shown in Fig. 2, anterior medial regions of atrophy encompassed CA2, CA3, and DG, whereas more extensive damage was observed laterally in CA1 and, in contrast to HYP patients, also in the lateral CA2 region. The inferior surface of the P map showed significant prosubicular atrophy anteriorly.

The HYP contralateral P map displayed a few discrete regions of atrophy (Fig. 6, left column) on the superior and inferior surfaces. However, the proportion of surface points exhibiting atrophy in the HYP contralateral P map was not statistically significant, a finding consistent with results of the paired *t*-tests described previously, which showed no significant difference in contralateral hippocampal volumes between HYP patients and control subjects.

In patients with LVF seizure onsets, atrophy in the contralateral hippocampus was distributed in lateral areas containing CA1. This pattern of atrophy was similar to that observed in the ipsilateral P maps, but extended more posteriorly (Fig. 6, right column). The extent of this damage is better illustrated if the P map is rotated 90 degrees to fully reveal the lateral aspect of the hippocampus. Examination of the inferior surface also revealed subicular atrophy along the medial edge of the hippocampus, as well as limited anterior prosubicular atrophy.

Nine of the 16 patients proceeded to epilepsy surgery, and eight of the nine patients had anteromesial temporal lobe resection, whereas one patient with HYP onsets had a temporoparietal neocortical resection. Follow-up interviews to assess surgical outcome revealed that two of three patients with HYP onsets (follow up after surgery, 3.2 ± 1.5 years) were free of disabling seizures, that is, Engel class I (Engel, 1987), whereas the remaining HYP onset patient who had a neocortical resection showed no improvement following surgery (class IV). Three of six patients with LVF onsets (4.7 ± 1.8 years) had class I outcomes, and the remaining three patients had a worthwhile reduction in seizure frequency (class III).

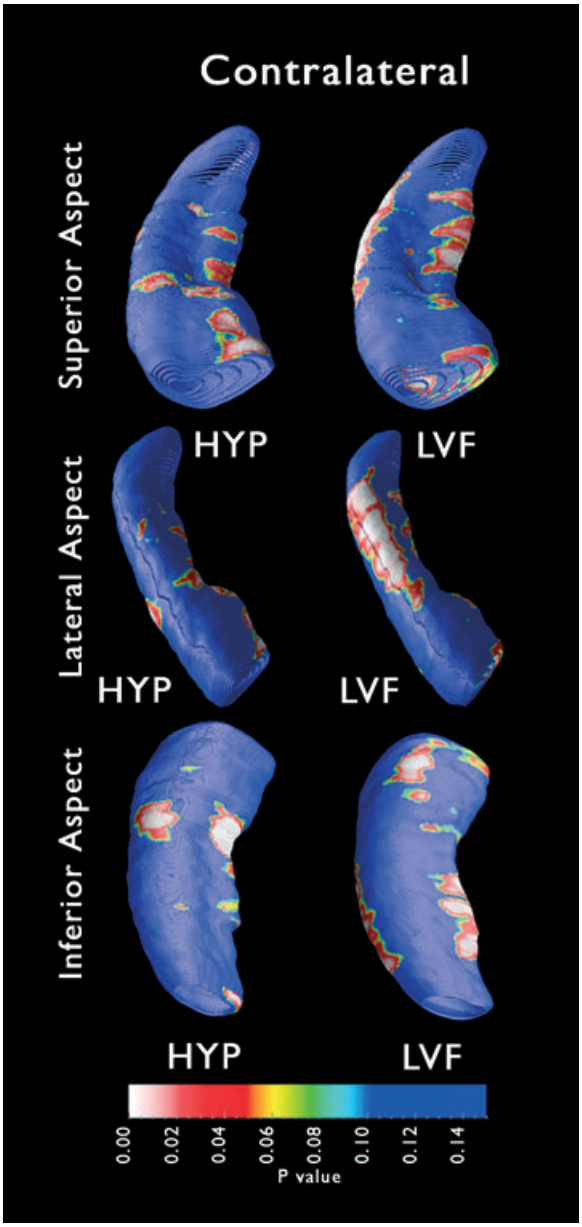

Figure 6.
Structural changes in contralateral hippocampus: Mapping three-dimensional (3D) hippocampal atrophy. Surface contour maps depicting areas of local atrophy (P maps) show regions of significant differences in HYP (n = 6) and LVF (n = 9) patients relative to controls. White and red indicate areas of significant atrophy ($p < 0.05$), whereas blue indicates areas without significant atrophy ($p > 0.10$). The HYP P map (left column), which exhibits some localized regions of medial atrophy, was not found to be significant (HYP $p < 0.064$). On this P map, the proportion of surface points with significant p-values was no higher than might be observed by chance. Significant levels of local atrophy relative to controls were observed only in the LVF patient group (LVF $p < 0.044$). The LVF P map (right column) depicts some medial atrophy, as well as significant lateral atrophy, which is best visualized when the P map displaying the superior aspect (right, top) is rotated 90 degrees to expose the lateral aspect (right, middle).

Data derived from histologic analysis of resected epileptogenic hippocampal tissue were available for six of eight patients who had anteromesial temporal lobe resection (one HYP and five LVF onsets). Based on criteria from Mathern et al. (2002), in which HS is defined as extensive neuron loss and gliosis throughout the hippocampus, with the most substantial damage in CA4, CA1, and prosubiculum, a diagnosis of HS was made in the one patient with HYP onsets, and in four of five patients with LVF onsets. The one remaining patient with LVF onsets was diagnosed non-HS.

Discussion

In contrast to the HYP group, which showed only ipsilateral atrophy, our volume data showed that patients with LVF ictal onsets exhibited significant bilateral HA. In addition, 3D hippocampal contour maps revealed that a distinct distribution of ipsilateral atrophy was associated with each onset group.

Although significant ipsilateral HA was present in both groups of patients, only the HYP group exhibited a pattern of atrophy typical of classical HS. Areas of local atrophy observed on the HYP P map likely reflect cell loss in CA1, CA3, CA4, DG, and prosubiculum. The possibility of cell loss in these hippocampal subfields is consistent with results from previous histologic studies (Townsend & Engel, 1991; Spencer et al., 1992b; Velasco et al., 2000), and agrees with the diagnosis of HS in one patient with HYP onsets in the present study. There was noticeably less atrophy in lateral areas on the group P map, which likely correspond to CA2. CA2 sparing is characteristic of classical HS as described by Bratz (1899), a common pathologic finding associated with mesial temporal lobe epilepsy (MTLE) (Engel, 1996a).

In contrast, much of the lateral atrophy observed ipsilaterally in LVF patients likely reflects cell loss within CA2. The absence of age-matched autopsy material precludes an accurate quantification of neuronal loss in the present study, but the group P maps would predict extensive CA2 damage in patients with LVF onsets. Indeed, Velasco et al. (2000) showed greater or equivalent cell loss in CA2 compared to all hippocampal subfields, except CA1, in patients with LVF onsets. This atypical distribution of damage in the LVF group appears more diffuse than classical HS and could result from the influence of extrahippocampal epileptogenic regions. Indeed, LVF activity is similar to the recruiting rhythm of neocortical seizures and is usually associated with extrahippocampal ictal onsets (Engel, 1996a, 2001), and neocortical areas have been shown to be significantly damaged in many patients with TLE who also exhibit HA (Lin et al., 2007). Furthermore, voltage depth profile analysis has shown that the peak amplitudes of LVF onsets are located in the lateral temporal lobe, indicating neocortical, as opposed to mesial temporal, regions of ictal onset (Bragin et al., 2005b). Future studies examining neocortical atrophy in HYP and LVF patient groups may help to establish the extent of extrahippocampal damage associated with each type of seizure onset.

The different patterns of ipsilateral HA we observed in patients with HYP or LVF seizure onsets were based on hippocampal MRI data from 16 patients, acquired using a single MR scanner, and from 19 control subjects, using a different scanner. Several studies have shown that neither manual nor automatic segmentation of mesial temporal structures is affected significantly by interscanner variability (Briellmann et al., 2001; Stonnington et al., 2008). In the present study, however, the use of different scanners may have contributed to some variability between patients and controls, but it is unlikely to have had much of an effect on our analysis between patient groups. It should also be noted that because the objective of this study was to characterize ipsilateral and contralateral HA with respect to seizure-onset morphology, we combined left and right hippocampi of female and male patients, grouping hippocampi solely on the basis of relation to side of seizure onset. This was done in part to maximize our sample size and statistical power, in order to detect differences between HYP and LVF groups, but also because studies show that the occurrence and severity of HS in patients with seizure disorders appear to be unrelated to gender and hemisphere (Briellmann et al., 1999).

In MTLE, seizure origin characteristically involves the hippocampal formation. Unlike seizures that originate in temporal neocortex and spread quickly to the frontal lobes and contralateral temporal lobe (Lieb et al., 1991), hippocampal onset seizures are usually more focal and tend to remain confined to the epileptogenic region, failing to propagate outside the ipsilateral hippocampus, or doing so only after an extended period of seconds or even several minutes (Lieb et al., 1987). In the present study, much of the atrophy distributed within medial regions of the ipsilateral hippocampi of patients with HYP onsets likely represents cell loss in CA4 and/or CA3. Damage to excitatory and inhibitory networks in this region may affect transmission through the DG-CA3-CA1 pathway, which may produce synchronous discharges resulting in large amplitude spiking similar to a HYP onset pattern. Seizures generated in the hippocampus typically exhibit HYP ictal-onset patterns, and often spread contralaterally only after transitioning to LVF activity or another type of ictal-discharge pattern (Engel, 1996a; Bragin et al., 1999). The restriction of HA to the ipsilateral hippocampus in the HYP group may reflect the focal nature of HYP onset seizures and their failure to escape the hippocampus.

The contralateral atrophy observed in LVF patients, however, may be evidence of a bilateral temporal lobe disorder, predisposing the group to rapid contralateral propagation. Although all LVF patients in the current study

were determined to have unilateral ictal onsets based on a dataset limited by short hospital stays, areas of contralateral HA are not adequately explained by longer duration of epilepsy or greater frequency of seizures compared to patients with HYP onsets, but could reflect the presence of undetected secondary epileptogenic regions. Alternatively, the contralateral HA of the LVF group could also reflect damage resulting from long-term exposure to propagated ictal activity via a pathway that involves entorhinal cortex. LVF seizure onsets, unlike HYP onsets, often start simultaneously in the entorhinal cortex and hippocampus in patients with TLE (Spencer & Spencer, 1994), as well as in the rodent kainic acid model of TLE (Bragin et al., 2005a). It has been shown that in nonhuman primates the entorhinal cortex projects to the contralateral subiculum (Amaral et al., 1984), so it is plausible that the contralateral subicular atrophy observed in the present study may reflect a pathway by which LVF ictal discharges within ipsilateral entorhinal cortex spread to contralateral subiculum and surrounding hippocampal areas. Although there is generally relatively little cell loss within the ipsilateral subiculum in patients with TLE (Bratz, 1899; Mathern et al., 1995a), MRI studies (Hogan et al., 2004) and histologic analysis of autopsy tissue (Mathern et al., 1995b) have shown that the contralateral subiculum may be damaged in patients with TLE.

The bilateral hippocampal damage we observed in the LVF group may also help explain why our finding of significant and nearly equal ipsilateral volume reductions in both HYP and LVF ictal-onset groups differs from the findings of histologic studies. Although previous studies have shown that both ictal onset patterns occur in the presence of HA (Spencer et al., 1992b; Spanedda et al., 1997; Velasco et al., 2000), cell loss was typically found to be greater in HYP patients than in patients with LVF onsets. However, these studies included only patients who went to surgery, and for whom tissue was available for analysis. Because LVF onsets are more likely to be regional as opposed to focal, and are associated with more diffuse, bilateral atrophy, LVF patients with more extensive damage may be less likely to be surgical candidates, and thus, less likely to be available for histologic evaluation. In contrast, in the present study, we analyzed data from all patients characterized as HYP or LVF, whether or not surgical resection was carried out, and thus included some patients who would not have been represented in the histologic studies cited previously.

The noninvasive nature of our MRI structural analysis allowed us to examine hippocampal differences in a wider range of patients than are included in most seizure-onset morphology studies, and the use of normal controls provided a basis for interpreting those differences. The identification of specific group differences in the distribution of atrophy helps to further establish HYP and LVF ictal onsets as two separate phenomena, and supports the hypothesis that each is associated with a distinct mechanism of generation. The classical HS observed ipsilateral to the region of seizure onset in HYP patients is characteristic of MTLE, a syndrome in which seizures arise from pathologic alterations within intrahippocampal circuitry. In contrast, the distribution of bilateral HA in LVF patients suggests the involvement of extrahippocampal regions in seizure genesis and may indicate a more diffuse temporal lobe disorder distinct from classical MTLE with HS.

Acknowledgments

This work was supported by NIH grants NS-02808 and NS-33310. We gratefully acknowledge the contributions of Dr. Noriko Salamon for establishing the tracing protocol, Dr. Gary W. Mathern for histologic data, and Eric Behnke for technical assistance with these research studies.

We confirm that we have read the Journal's position on issues involved in ethical publication and affirm that this report is consistent with those guidelines.

None of the authors has any conflict of interest to disclose.

References

Amaral DG, Insausti R, Cowan WM. (1984) The commissural connections of the monkey hippocampal formation. *J Comp Neurol* 224:307–336.

Apostolova LG, Dutton RA, Dinov ID, Hayashi KM, Toga AW, Cummings JL, Thompson PM. (2006) Conversion of mild cognitive impairment to Alzheimer disease predicted by hippocampal atrophy maps. *Arch Neurol* 63:693–699.

Ballmaier M, Narr KL, Toga AW, Elderkin-Thompson V, Thompson PM, Hamilton L, Haroon E, Pham D, Heinz A, Kumar A. (2008) Hippocampal morphology and distinguishing late-onset from early-onset elderly depression. *Am J Psychiatry* 165:229–237.

Bearden CE, Thompson PM, Dutton RA, Frey BN, Peluso MA, Nicoletti M, Dierschke N, Hayashi KM, Klunder AD, Glahn DC, Brambilla P, Sassi RB, Mallinger AG, Soares JC. (2008) Three-dimensional mapping of hippocampal anatomy in unmedicated and lithium-treated patients with bipolar disorder. *Neuropsychopharmacology* 33:1229–1238.

Bragin A, Engel J Jr, Wilson CL, Vizentin E, Mathern GW. (1999) Electrophysiologic analysis of a chronic seizure model after unilateral hippocampal KA injection. *Epilepsia* 40:1210–1221.

Bragin A, Azizyan A, Almajano J, Wilson CL, Engel J Jr. (2005a) Analysis of chronic seizure onsets after intrahippocampal kainic Acid injection in freely moving rats. *Epilepsia* 46:1592–1598.

Bragin A, Wilson CL, Fields T, Fried I, Engel J Jr. (2005b) Analysis of seizure onset on the basis of wideband EEG recordings. *Epilepsia* 46(Suppl. 5):59–63.

Bratz E. (1899) Ammonshornbefunde bei epileptikern. *Arch Psychiatr Nervenkr* 31:820–835.

Briellmann RS, Jackson GD, Mitchell LA, Fitt GJ, Kim SE, Berkovic SF. (1999) Occurrence of hippocampal sclerosis: is one hemisphere or gender more vulnerable? *Epilepsia* 40:1816–1820.

Briellmann RS, Syngeniotis A, Jackson GD. (2001) Comparison of hippocampal volumetry at 1.5 tesla and at 3 tesla. *Epilepsia* 42:1021–1024.

Collins DL, Neelin P, Peters TM, Evans AC. (1994) Automatic 3D intersubject registration of MR volumetric data in standardized Talairach space. *J Comput Assist Tomogr* 18:192–205.

Crandall PH, Walter RD, Rand RW. (1963) Clinical applications of studies on stereotactically implanted electrodes in temporal-lobe epilepsy. *J Neurosurg* 20:827–840.

Edgington ES. (1995) *Randomization tests*. M. Dekker, New York.

Engel J Jr. (1987) Outcome with respect to epileptic seizures. In Engel J Jr. (Ed) *Surgical treatment of the epilepsies*. Raven Press, New York, pp. 553–571.

Engel J Jr. (1990) The Hans Berger lecture. Functional explorations of the human epileptic brain and their therapeutic implications. *Electroencephalogr Clin Neurophysiol* 76:296–316.

Engel J Jr. (1996a) Introduction to temporal lobe epilepsy. *Epilepsy Res* 26:141–150.

Engel J Jr. (1996b) Surgery for seizures. *N Engl J Med* 334:647–652.

Engel J Jr. (2001) Mesial temporal lobe epilepsy: what have we learned? *Neuroscientist* 7:340–352.

Fried I, Wilson CL, Maidment NT, Engel J Jr, Behnke E, Fields TA, MacDonald KA, Morrow JW, Ackerson L. (1999) Cerebral microdialysis combined with single-neuron and electroencephalographic recording in neurosurgical patients. Technical note. *J Neurosurg* 91:697–705.

Frisoni GB, Sabattoli F, Lee AD, Dutton RA, Toga AW, Thompson PM. (2006) In vivo neuropathology of the hippocampal formation in AD: a radial mapping MR-based study. *Neuroimage* 32:104–110.

Hogan RE, Wang L, Bertrand ME, Willmore LJ, Bucholz RD, Nassif AS, Csernansky JG. (2004) MRI-based high-dimensional hippocampal mapping in mesial temporal lobe epilepsy. *Brain* 127:1731–1740.

Lepore N, Shi Y, Lepore F, Fortin M, Voss P, Chou YY, Lord C, Lassonde M, Dinov ID, Toga AW, Thompson PM. (2008) Patterns of hippocampal shape and volume differences in blind subjects. *Neuroimage* (in press).

Lieb JP, Engel J Jr, Brown WJ, Gevins AS, Crandall PH. (1981) Neuropathological findings following temporal lobectomy related to surface and deep EEG patterns. *Epilepsia* 22:539–549.

Lieb JP, Hoque K, Skomer CE, Song XW. (1987) Inter-hemispheric propagation of human mesial temporal lobe seizures: a coherence/phase analysis. *Electroencephalogr Clin Neurophysiol* 67:101–119.

Lieb JP, Dasheiff RM, Engel J Jr. (1991) Role of the frontal lobes in the propagation of mesial temporal lobe seizures. *Epilepsia* 32:822–837.

Lin JJ, Salamon N, Dutton RA, Lee AD, Geaga JA, Hayashi KM, Toga AW, Engel J Jr, Thompson PM. (2005) Three-dimensional preoperative maps of hippocampal atrophy predict surgical outcomes in temporal lobe epilepsy. *Neurology* 65:1094–1097.

Lin JJ, Salamon N, Lee AD, Dutton RA, Geaga JA, Hayashi KM, Luders E, Toga AW, Engel J Jr, Thompson PM. (2007) Reduced neocortical thickness and complexity mapped in mesial temporal lobe epilepsy with hippocampal sclerosis. *Cereb Cortex* 17:2007–2018.

Mai JK, Assheuer J, Paxinos G. (2004) *Atlas of the human brain*. Elsevier Academic Press, San Diego.

Margerison JH, Corsellis JA. (1966) Epilepsy and the temporal lobes. A clinical, electroencephalographic and neuropathological study of the brain in epilepsy, with particular reference to the temporal lobes. *Brain* 89:499–530.

Mathern GW, Pretorius JK, Babb TL. (1995a) Quantified patterns of mossy fiber sprouting and neuron densities in hippocampal and lesional seizures. *J Neurosurg* 82:211–219.

Mathern GW, Pretorius JK, Babb TL, Quinn B. (1995b) Unilateral hippocampal mossy fiber sprouting and bilateral asymmetric neuron loss with episodic postictal psychosis. *J Neurosurg* 82:228–233.

Mathern GW, Adelson PD, Cahan LD, Leite JP. (2002) Hippocampal neuron damage in human epilepsy: Meyer's hypothesis revisited. *Prog Brain Res* 135:237–251.

Narr KL, Thompson PM, Szeszko P, Robinson D, Jang S, Woods RP, Kim S, Hayashi KM, Asunction D, Toga AW, Bilder RM. (2004) Regional specificity of hippocampal volume reductions in first-episode schizophrenia. *Neuroimage* 21:1563–1575.

Nichols TE, Holmes AP. (2002) Nonparametric permutation tests for functional neuroimaging: a primer with examples. *Hum Brain Mapp* 15:1–25.

Nicolson R, DeVito TJ, Vidal CN, Sui Y, Hayashi KM, Drost DJ, Williamson PC, Rajakumar N, Toga AW, Thompson PM. (2006) Detection and mapping of hippocampal abnormalities in autism. *Psychiatry Res* 148:11–21.

Portney LG, Watkins MP. (2008) Statistical measures of reliability. In *Foundations of clinical research: applications to practice*. Pearson/Prentice Hall, Upper Saddle River, NJ, pp. 585–618.

Spanedda F, Cendes F, Gotman J. (1997) Relations between EEG seizure morphology, interhemispheric spread, and mesial temporal atrophy in bitemporal epilepsy. *Epilepsia* 38:1300–1314.

Spencer SS, Guimaraes P, Katz A, Kim J, Spencer D. (1992a) Morphological patterns of seizures recorded intracranially. *Epilepsia* 33:537–545.

Spencer SS, Kim J, Spencer DD. (1992b) Ictal spikes: a marker of specific hippocampal cell loss. *Electroencephalogr Clin Neurophysiol* 83:104–111.

Spencer SS, Spencer DD. (1994) Entorhinal-hippocampal interactions in medial temporal lobe epilepsy. *Epilepsia* 35:721–727.

Stonnington CM, Tan G, Kloppel S, Chu C, Draganski B, Jack CR Jr, Chen K, Ashburner J, Frackowiak RS. (2008) Interpreting scan data acquired from multiple scanners: a study with Alzheimer's disease. *Neuroimage* 39:1180–1185.

Thompson PM, Schwartz C, Toga AW. (1996) High-resolution random mesh algorithms for creating a probabilistic 3D surface atlas of the human brain. *Neuroimage* 3:19–34.

Thompson PM, Hayashi KM, de Zubicaray G, Janke AL, Rose SE, Semple J, Herman D, Hong MS, Dittmer SS, Doddrell DM, Toga AW. (2003) Dynamics of gray matter loss in Alzheimer's disease. *J Neurosci* 23:994–1005.

Thompson PM, Hayashi KM, De Zubicaray GI, Janke AL, Rose SE, Semple J, Hong MS, Herman DH, Gravano D, Doddrell DM, Toga AW. (2004) Mapping hippocampal and ventricular change in Alzheimer disease. *Neuroimage* 22:1754–1766.

Townsend JB, Engel J Jr. (1991) Clinicopathological correlations of low voltage fast and high amplitude spike and wave mesial temporal stereoencephalographic ictal onsets. *Epilepsia* 32:21.

Velasco AL, Wilson CL, Babb TL, Engel J Jr. (2000) Functional and anatomic correlates of two frequently observed temporal lobe seizure-onset patterns. *Neural Plast* 7:49–63.

Watson C, Andermann F, Gloor P, Jones-Gotman M, Peters T, Evans A, Olivier A, Melanson D, Leroux G. (1992) Anatomic basis of amygdaloid and hippocampal volume measurement by magnetic resonance imaging. *Neurology* 42:1743–1750.